

https://doi.org/10.1070/QEL16606

Diamond Raman laser emitting at 1194, 1419, and 597 nm

V.P. Pashinin, V.G. Ralchenko, A.P. Bolshakov, E.E. Ashkinazi, V.I. Konov

Abstract. **A Raman laser based on a synthetic diamond crystal pumped by nanosecond pulses of a 1030-nm Yb:YAG laser and emitting in the IR region at the first and second Stokes wavelengths of 1194 and 1419 nm, respectively, was developed. The conversion efficiency was 34% with a slope efficiency of 50% and an average power of 1.1 W at a wavelength of 1194 nm; the average power at 1419 nm was 0.52 W. Frequency doubling of the first Stokes component in a nonlinear BBO crystal resulted in orange (597.3 nm) radiation with a pulse energy of 0.15 mJ, an average power of 0.22 W, and a maximum efficiency of 20%.**

Keywords: *Raman laser, diamond, orange laser, second harmonic generation.*

1. Introduction

Diamond Raman lasers have recently attracted attention due to the unique combination of optical, thermophysical, and mechanical properties of diamond, which make it possible to achieve high powers of radiation in various spectral regions, from UV to mid-IR [1–8]. Diamond has the highest thermal conductivity among all bulk materials (up to 2300 W mK^{-1} at room temperature [9] and to 3300 W mK^{-1} for diamond enriched with ^{12}C isotope [10,11]), high transparency in the range from UV (225 nm) to radio waves [12], low thermal expansion coefficient (0.8×10^{-6} K^{-1} at $T = 273$ K), high chemical durability, and record-high hardness (80 GPa). A large Raman shift in diamond ($\nu = 1332$ cm^{-1}) makes it possible to vary the Raman laser wavelength in a wide range using, in particular, high-order Stokes and anti-Stokes components [2, 13, 14]. A high Raman gain in diamond (in particular, $g =$ 42 cm GW^{-1} for pumping at a wavelength $\lambda_p = 532$ nm and 12–17 cm GW^{-1} at $\lambda_p = 1064$ nm [15, 16]) allows fabrication of high-power Raman lasers even using small-size crystals, usually below 10 mm. The average output power of available Raman lasers based on traditional crystals is limited by about 5 W due to problems with heat removal and, as a result, with the appearance of a thermal lens, deterioration of the beam quality, and even mechanical breakdown of the material. Owing to the high thermal conductivity of diamond, these problems in diamond Raman lasers are much less pronounced, which makes it possible to considerably increase the radiation power.

At present, chemical vapour deposition (CVD) makes it possible to synthesise high-purity single crystals that can be used in optics and laser engineering [17–21], because of which almost all diamond Raman lasers are based on CVD diamonds. The authors of [22] demonstrated a diamond Raman laser with a power of 24.5 W emitting (without appearance of a thermal lens) at a wavelength of 1193 nm under pumping by a pulsed cryogenic Yb:YAG laser ($\tau_p = 75$ ns, $\lambda_p = 1030$ nm). Even higher powers were achieved in a quasi-cw regime (higher than 100 W at a wavelength of 1240 nm (first Stokes) under pumping by a microsecond Nd:YAG laser [23]) and in a cw regime (114 W at a wavelength of 1490 nm (second Stokes) with a conversion efficiency of 44% [24]).

Concerning the yellow-orange region (570–625 nm), in which the development of high-power high-efficiency lasers is a challenging task, operation of a diamond Raman laser at a wavelength of 573 nm (first Stokes) was achieved with a power of 1.2 W and a conversion efficiency of 63.5% under pumping by nanosecond pulses ($\lambda_p = 532$ nm), while the power at 620 nm (second Stokes) was an order of magnitude lower [25].

Laser radiation at wavelengths close to 600 nm is of interest for several applications. First, this radiation is used to form laser guide stars (LGSs) for astronomical telescope adaptive optics [26]. The laser is used to form a luminous point – LGS, i.e., to excite fluorescence of sodium atoms at a height of 90 km in the atmosphere, where these atoms exist in natural form. Measurements of the LGS emission allow one to correct aberrations caused by the Earth's atmosphere in the images of real stars by adaptive optics. Sodium atoms can be excited by a laser beam with a wavelength of the D2 line (589.2 nm) and emit at the same wavelength thus forming a bright fluorescent source exactly at the desired distance [27]. Second, orange light sources can be used for efficient (resonance) excitation of photoluminescence (PL) of a new germanium–vacancy (GeV) colour centre in diamond, which has a PL line at a wavelength of 602 nm and is of interest for application in optical quantum technologies [28, 29].

A finer wavelength adjustment can be achieved by using isotopically modified diamonds grown with a prescribed ratio

V.P. Pashinin A.M. Prokhorov General Physics Institute, Russian Academy of Sciences, ul. Vavilova 38, 119991 Moscow, Russia; 38; e-mail: pash@nsc.gpi.ru;
V.G. Ralchenko, A.P. Bolshakov A.M. Prokhorov General Physics Institute, Russian Academy of Sciences, ul. Vavilova 38, 119991 Moscow, Russia; National Research Nuclear University 'MEPhI', Kashirskoe sh. 31, 115409 Moscow, Russia; Harbin Institute of Technology, 150080 Harbin, P.R. China;
e-mail: vg_ralchenko@mail.ru, bolshak@ran.gpi.ru;
E.E. Ashkinazi, V.I. Konov A.M. Prokhorov General Physics Institute, Russian Academy of Sciences, ul. Vavilova 38, 119991 Moscow, Russia; National Research Nuclear University 'MEPhI', Kashirskoe sh. 31, 115409 Moscow, Russia; e-mail: ashkinazi@nsc.gpi.ru, konov@nsc.gpi.ru

Received 25 December 2017
Kvantovaya Elektronika **48** (3) 201–205 (2018)
Translated by M.N. Basieva

of ^{12}C and ^{13}C isotopes (the difference between the frequencies of the first-order Raman lines for diamonds with 100% concentrations of ^{12}C and ^{13}C isotopes is 51 cm^{-1}) [11, 30]. Orange lasers are also important for biomedical investigations, in particular, in cytometry, because some important luminescent proteins are most efficiently excited at wavelengths of 590–595 nm [31].

In the present work, we report a Raman laser based on single-crystal CVD diamond pumped by a nanosecond Yb:YAG laser (λ_p = 1030 nm) and emitting at the first and second Stokes wavelengths (1194 and 1419 nm, respectively), as well as in the orange spectral range at 597.3 nm due to second harmonic generation of the first Stokes.

2. Optical scheme of the Raman laser

The optical scheme of the diamond Raman laser, which is similar to that used by us previously with pumping by a Nd:YAG laser [6], is shown in Fig. 1. Pumping was performed by a laser based on an Yb:YAG crystal with a size of 5×5×1 mm and an Yb concentration of 10 wt%, which, in turn, was pumped by an FBLD-940-200-FC200 (Frankfurt Laser) fibre-coupled diode laser with the following parameters: maximum output power 200 W, optical fibre diameter 200 μm, numerical aperture 0.22, and pulse duration 300–350 μs. The Yb:YAG laser parameters were as follows: TEM_{00} mode, pulse duration at half maximum 12 ns, beam diameter at the output mirror 0.5 mm, and divergence 3 mrad. With increasing pump pulse repetition rate, the pump pulse energy decreased from E = 2.9 mJ at the rate f = 100 Hz to 2.2 mJ at f = 1500 Hz. The maximum average output P_p of this laser at λ_p = 1030 nm was 3.2 W.

The Yb:YAG laser beam was focused using mirror M1 and lens L1 (F = 100 mm) into the CVD-diamond crystal in the cavity formed by concave mirror M2 (R = 100 mm) and plane output mirror M_{out}. A CVD-diamond plate 7.8×7.8×1.0 mm in size with all faces polished (the crystal was grown using microwave plasma, impurity nitrogen concentration was about 1 ppm) had large faces with the (100) orientation and the other (narrow) faces with the (110) orientation. The pump radiation propagated in the (110) direction parallel to the long edge of the crystal. The faces of the diamond plate were coated with an antireflective film to achieve the reflectance below 0.3% for the range of 1020–1440 nm. The direction of the pump polarisation vector was changed using a half-wave plate. The crystal was attached to a copper heat sink with thermal grease.

The M2 mirror transmittance at wavelength λ_p = 1030 nm was 90%. The pump beam diameter in the focal plane of the lens approximately coincided with the diameter of the TEM_{00} cavity mode (280 μm). Modelling with the LasCAD software showed that the chosen cavity configuration, which is close to semi-confocal, yields a more stable diameter of the fundamental mode in the case of appearance of a thermal lens in the diamond crystal than the semi-spherical cavity. Faraday rotator F and polariser P placed between the Yb:YAG laser and the Raman laser cavity did not allow the reflected pump radiation to return into the Yb:YAG laser cavity. As an output mirror, we used M_{out} mirror with a dielectric coating having different transmission spectra in the range of 1030–1419 nm. The transmittances of the output mirrors at the wavelengths of pump radiation and the first and second Stokes in diamond are listed in Table 1.

The energies of pump and Raman laser pulses were measured by an Ophir PE-09 pyroelectric detector connected to a computer via an Ophir Juno USB interface. The shapes of the pump and Raman laser pulses were recorded using a Teledyne LeCroy Wave Surfer 10R oscilloscope (bandwidth 1 GHz)

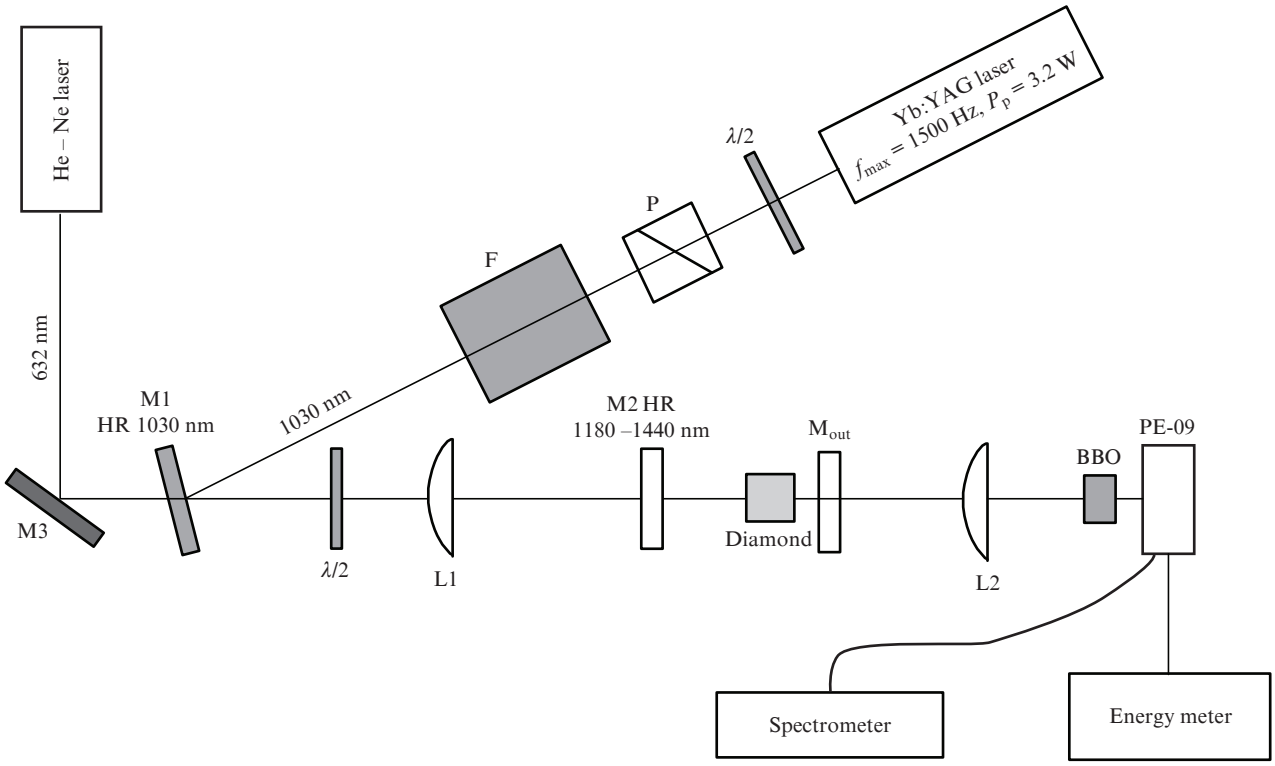

Figure 1. Optical scheme of the Raman laser pumped by an Yb:YAG laser.

Table 1. Transmittance T (%) of output mirrors M_{out} for different wavelengths.

Mirror number	Wavelength/nm		
	1030	1194	1419
1	<0.1	77	84
2	0.15	0.4	92

and a Thorlabs DET 025A photodiode (response time 150 ps). The spectral characteristics of the pump and Raman laser radiation were studied using an M150-III monochromator and an UC-16H914 InGaAs linear detector (Solar LS). The radiation was delivered to the input slit of the monochromator through an optical fibre. The nominal spectral resolution of the monochromator was 0.6 nm with a 600-line mm^{-1} diffraction grating and 0.3 nm with a 1200-line mm^{-1} grating (for recording the second harmonic of the Raman laser).

3. IR lasing

Dependences of the output pulse energy and power of the Raman laser at a wavelength of 1194 nm (first Stokes, Mirror M_{out} No. 1) on the energy and average power of the Yb:YAG pump laser are presented in Fig. 2. The threshold pump energy was about 0.7 mJ and the maximum pulse energy was 0.75 mJ with a maximum conversion efficiency $\eta = 34\%$ and a slope efficiency $\eta_d = 50\%$ (Fig. 2a). The maximum value of η was achieved with pump radiation polarised at an angle of 45° to the diamond crystal faces, i.e., with the polarisation vector lying in the (111) plane.

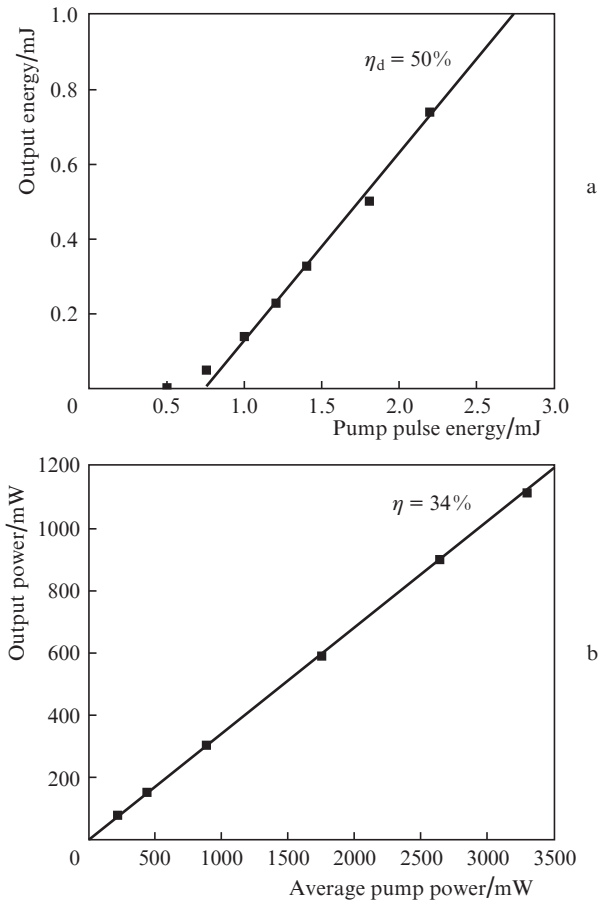

Figure 2. Dependences of the (a) output pulse energy and (b) average power of the Raman laser at a wavelength of 1194 nm (first Stokes) on, respectively, the pump Yb:YAG laser pulse energy and power (at a constant pump pulse energy of 2.2 mJ).

An increase in the average pump power due to increasing pulse repetition rate (with an unchanged pump pulse energy of 2.2 mJ) leads to a linear increase in the output Raman laser power (Fig. 2b). With this method of changing the pump power, the threshold Raman laser power was formally close to zero. The maximum average output power at a wavelength of 1194 nm was 1.1 W with a conversion efficiency $\eta = 34\%$. The Raman laser wavelength in the maximum was 1193±0.6 nm, which corresponds to the first Stokes frequency in diamond (1332 cm^{-1}); the spectrum FWHM was ~1 nm (Fig. 3). The pulse duration (FWHM) was about 10 ns (Fig. 4).

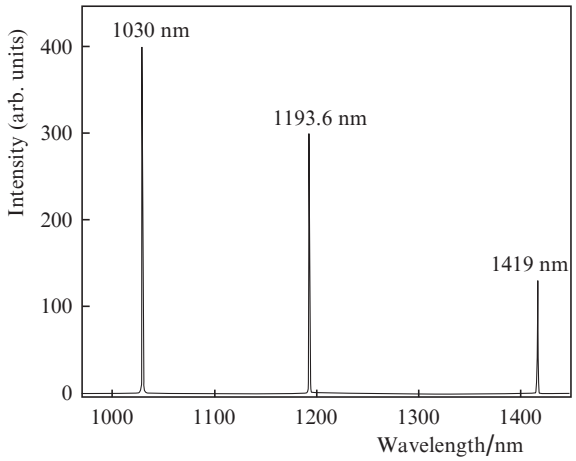

Figure 3. Spectra of the pump laser (λ = 1030 nm) and the Raman laser at the first (1193.6 nm) and second (1419 nm) Stokes lines.

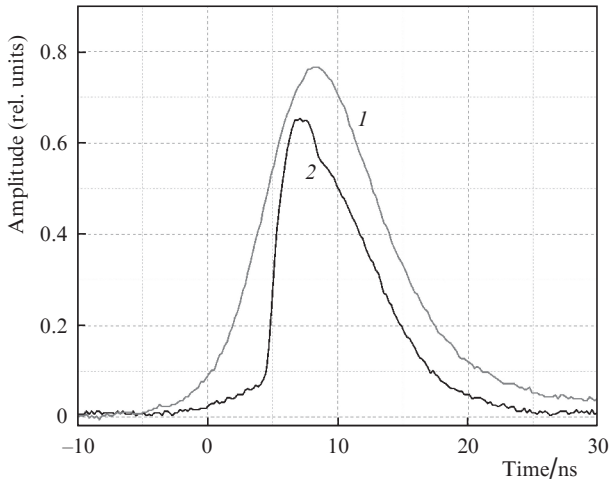

Figure 4. Oscillograms of (*1*) pump and (*2*) Raman (λ = 1194 nm) pulses with output mirror M_{out} No. 1.

In the case of mirror M_{out} No. 2 with a high ($R > 99\%$) reflectance at a wavelength of 1194 nm, the Raman laser emitted at the second Stokes wavelength (1419 nm) (Fig. 3). The FWHM of the 1419-nm line was 1.2 nm. The dependence of the Raman laser pulse energy (λ = 1419 nm) on the pump pulse energy is shown in Fig. 5. With increasing pump pulse repetition rate up to 1500 Hz, the output Raman laser power

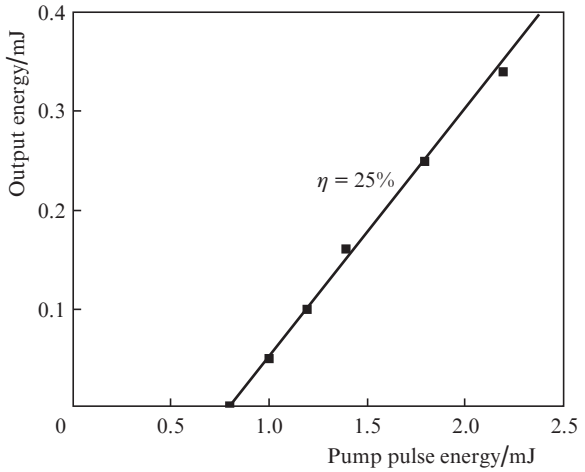

Figure 5. Dependence of the Raman pulse energy (λ = 1419 nm) on the pump pulse energy.

(λ = 1419 nm) linearly increases with increasing pump power without a tendency to saturation. The slope efficiency η_d was 25%, while the maximum average output power of the first-Stokes radiation reached 0.52 W. Further increase in the output Raman laser power can be achieved by increasing the pulse repetition rate, which is possible after improving the cooling scheme of the active element of the pump laser. Optimisation of the pump laser cavity Q-factor also will allow an increase in the total efficiency and average power.

4. Lasing in the orange spectral range

Orange emission of the Raman laser was achieved by frequency doubling of the Raman laser radiation in a nonlinear crystal. For second harmonic generation (SHG), we used a BaB_2O_4 (BBO) crystal measuring 6×6×3 mm and oriented for type-I SHG (θ = 21.2°). The 1194-nm radiation with a power of 1 W was focused by lens L2 with a focal length of 50 mm (see Fig. 1) into a spot 0.3 mm in diameter in the centre of the BBO crystal. The output energy and spectral characteristics were studied using the same metrological equipment as for the pump and Raman lasers, but the 600-line mm^{-1} grating with a blaze wavelength of 1000 nm in the M1150-III monochromator was replaced by a 1200-line mm^{-1} grating with a blaze wavelength of 400 nm.

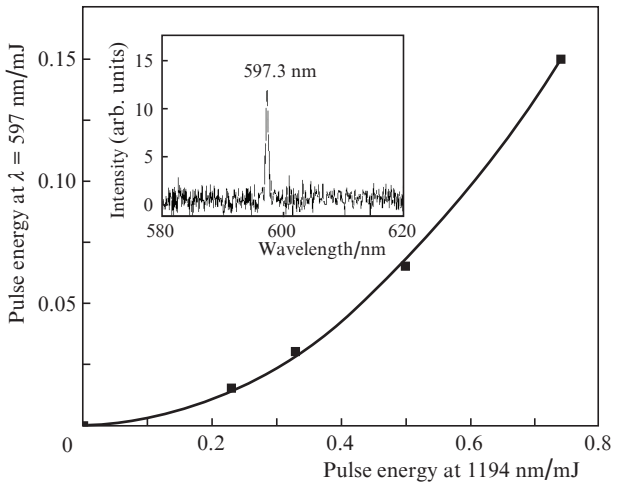

Figure 6. Dependence of the pulse energy of the second harmonic (λ = 597 nm) of the Raman laser on the pump (λ = 1194 nm) pulse energy. The inset shows the SHG spectrum peaking at λ = 597.3 nm.

The SHG spectrum and the quadratic dependence of the output Raman pulse energy on the pump pulse energy are shown in Fig. 6. The maximum energy achieved at a wavelength of 597.3 nm was 0.15 mJ, the maximum average power reached 220 mW, and the maximum efficiency was 20%. The spectral width of the orange laser radiation was measured to be 0.5 nm, which is close to the spectrometer resolution (0.3 nm).

5. Conclusions

We fabricated a Raman laser based on a synthetic diamond single crystal about 8 mm long. Under pumping by a nanosecond Yb:YAG laser (wavelength 1030 nm, average power up to 3.2 W, pulse duration about 10 ns), we obtained lasing at the first and second Stokes wavelengths, i.e., at 1194 and 1419 nm, respectively. The average output power at λ = 1194 nm reached 1.1 W with a conversion efficiency of 34% and a slope efficiency of 50%. The average output power at a wavelength of 1419 nm was 0.52 W. Doubling of the first Stokes frequency in a nonlinear BBO crystal resulted in orange laser radiation at 597.3 nm with a pulse energy of 0.15 mJ and an average power of 0.22 W. The output power for all the three laser frequencies in the IR and visible spectral ranges showed no tendency to saturation with increasing average pump power. This suggests that the Raman laser power can be further increased by increasing the pump power and optimising the cavity, keeping in mind that the record-high thermal conductivity (about 2000 W mK^{-1}) of diamond helps to decrease temperature gradients appearing in the crystal.

Acknowledgements. This work was supported by the Russian Science Foundation (Grant No. 14-12-01403-P).

References

1. Granados E., Spence D.J., Mildren R.P. *Opt. Express*, **19**, 10857 (2011).
2. Reilly S., Savitski V.G., Liu H., Gu E., Dawson M.D., Kemp A.J. *Opt. Lett.*, **40**, 930 (2015).
3. Jelínek M., Kitzler O., Jelínková H., Šulc J., Němec M. *Laser Phys. Lett.*, **9**, 35 (2012).
4. Feve J.P.M., Shortoff K.E., Bohn M.J., Brasseur J.K. *Opt. Express*, **19**, 913 (2011).
5. McKay A., Liu H., Kitzler O., Mildren R.P. *Laser Phys. Lett.*, **10**, 105801 (2013).
6. Pashinin V.P., Ralchenko V.G., Bolshakov A.P., Ashkinazi E.E., Gorbashova M.A., Yurov V.Y., Konov V.I. *Laser Phys. Lett.*, **13**, 065001 (2016).
7. Murtagh M., Lin J., Mildren R.P., McConnell G., Spence D.J. *Opt. Express*, **23**, 15504 (2015).
8. Sabella A., Piper J.A., Mildren R.P. *Opt. Lett.*, **39**, 4037 (2014).
9. Bolshakov A.P., Ralchenko V.G., Yurov V.Y., Popovich A.F., Antonova I.A., Khomich A.A., Ashkinazi E.E., Ryzhkov S.G., Vlasov A.V., Khomich A.V. *Diamond Relat. Mater.*, **62**, 49 (2016).
10. Wei L., Kuo P.R., Thomas R.L., Anthony T.R., Banholzer W.F. *Phys. Rev. Lett.*, **70**, 3764 (1993).
11. Kaminskii A.A., Ral'chenko V.G., Yoneda H., Bol'shakov A.P., Inyushkin A.V. *Pis'ma Zh. Eksp. Teor. Fiz.*, **104**, 356 (2016).
12. Mildren R.P., in *Optical Engineering of Diamond* (New York: Wiley, 2013) p.1.

13. Lux O., Ralchenko V.G., Bolshakov A.P., Konov V.I., Sharonov G.V., Shirakawa A., Yoneda H., Rhee H., Eichler H.J., Mildren R.P., Kaminskii A.A. *Laser Phys. Lett*., **11**, 086101 (2014).
14. Kaminskii A.A., Lux O., Ralchenko V.G., Bolshakov A.P., Rhee H., Eichler H.J., Shirakawa A., Yoneda H. *Phys. Stat. Solidi (RRL)-Rapid Res. Lett.*, **10**, 471 (2016).
15. Savitski V.G., Reilly S., Kemp A.J. *IEEE J. Quantum Electron.*, **49**, 218 (2013).
16. Kaminskii A.A., Hemley R.J., Lai J., Yan C.S., Mao H.K., Ralchenko V.G., Eichler H.J., Rhee H. *Laser Phys. Lett.*, **4**, 350 (2007).
17. Balmer R.S., Brandon J.R., Clewes S.L., Dhillon H.K., Dodson J.M., Friel I., Inglis P.N., Madgwick T.D., Markham M.L., Mollart T.P., Perkins N., Scarsbrook G.A., Twitchen D.J., Whitehead A.J., Wilman J.J., Woollard S.M. *J. Phys.: Cond. Matter*, **21**, 364221 (2009).
18. *Optical Engineering of Diamond* (New York: Wiley, 2013).
19. Konov V.I. *Quantum Electron*., **45**, 1043 (2015) [*Kvantovaya Elektron*., **45**, 1043 (2015)].
20. Ivakin E.V., Kiselev I.G., Ral'chenko V.G., Bol'shakov A.P., Ashkinazi E.E., Sharonov G.V. *Quantum Electron*., **44**, 1055 (2014) [*Kvantovaya Elektron*., **44**, 1055 (2014)].
21. Komlenok M.S., Volodkin B.O., Knyazev B.A., Kononenko V.V., Kononenko T.V., Konov V.I., Pavel'ev V.S., Soifer V.A., Tukmakov K.N., Choporova Yu.Yu. *Quantum Electron*., **45**, 933 (2015) [*Kvantovaya Elektron.*, **45**, 933 (2015)].
22. Feve J.P.M., Shortoff K.E., Bohn M.J., Brasseur J.K. *Opt. Express*, **19**, 913 (2011).
23. Williams R.J., Spence D.J., Lux O., Mildren R.P. *Opt. Express*, **25**, 749 (2017).
24. Mildren R.P., Butler J.E., Rabeau J.R. *Opt. Express*, **16**, 18950 (2008).
25. Mildren R.P., Sabella A. *Opt. Lett.*, **34**, 2811 (2009).
26. Bol'basova L.A., Lukin V.P. *Opt. Atmos. Okeana*, **22**, 807 (2009).
27. Bland-Hawthorn J., Kern P. *Opt. Express*, **17**, 1880 (2009).
28. Ral'chenko V.G., Sedov V.S., Khomich A.A., Krivobok V.S., Nikolaev S.N., Savin S.S., Vlasov I.I., Konov V.I. *Kratk. Soobshch. Fiz. FIAN*, No. 6, 15 (2015).
29. Iwasaki T., Ishibashi F., Miyamoto Y., Doi Y., Kobayashi S., Miyazaki T., Tahara K., Jahnke K.D., Rogers L.J., Naydenov B., Jelezko F., Yamasaki S., Nagamachi S., Inubushi T., Mizuochi N., Hatano M. *Sci. Rep*., **5**, 12882 (2015).
30. Vogelgesang R., Ramdas A.K., Rodriguez S., Grimsdich M., Anthony T.R. *Phys. Rev. B*, **54**, 3989 (1996).
31. Telford W.G., Illy E., Karlsson H., Prabhat P. *Biophoton. Intern*., **17**, 26 (2010).